

Lagrangian air-mass tracking with smart balloons during ACE-2

Randy Johnson

National Oceanic and Atmospheric Administration, Air Resources Laboratory, Field Research Division, Idaho Falls, Idaho 83402

Steven Businger and Annette Baerman

University of Hawaii, Honolulu, Hawaii 96822

ABSTRACT

A third-generation Smart Balloon designed at National Oceanic and Atmospheric Administration, Air Resources Laboratory Field Research Division, in collaboration with the University of Hawaii (UH), was released from ship-board during the recent Second Aerosol Characterization Experiment (ACE-2) to provide Lagrangian air-mass tracking data. ACE-2 is the third in a series of field experiments designed to study the chemical, physical, and radiative properties and processes of atmospheric aerosols and their role in climate and is organized by the International Global Atmospheric Chemistry (IGAC) program. The adjective *smart* in the title of this paper refers to the fact that the buoyancy of the balloon automatically adjusts through the act of pumping air into or releasing air from the ballast portion of the balloon when it travels vertically outside a barometric pressure range set prior to release. The smart balloon design provides GPS location, barometric pressure, temperature, relative humidity, and other data via a transponder to a C130 research aircraft flying in the vicinity of the balloon. The addition of two-way communication allows interactive control of the balloon operating parameters by an observer. A total of three cloudy Lagrangian experiments were conducted during the ACE-2 field program which lasted from 16 June through 26 July 1997. This paper reviews the design and capability of the smart balloons and their performance during the ACE-2 Lagrangian experiments. Future development and applications of the technology are discussed.

1. Introduction

A Lagrangian frame of reference, one that moves with the flow of the atmosphere, has been used for many years to track pollution and monitor the evolution of a parcel of air in the atmosphere (Seinfeld et al. 1973; Zack 1983, Businger et al. 1996). Some problems involving reactive trace species in the atmosphere are so complex that there is no substitute for observing their rates in the actual atmosphere. In Lagrangian experiments a volume of air is tagged and tracked over time, allowing scientists the opportunity to repeatedly make measurements in the same volume of air as it moves with the wind. These experiments are difficult to implement, but it is a powerful approach and the data collected in this way lend themselves to subsequent numerical modeling (e.g., Suhre et al. 1998).

The mean concentration budget for the a scalar variable in well mixed boundary layer can be written

$$\frac{dS}{dt} = \frac{(w_e \Delta S)_h}{h} + \frac{(\overline{w \phi})_0}{h} + K_i \left(\frac{\partial \bar{S}}{\partial x_i} \right)^2 + Q_s. \quad (1)$$

where the horizontal advection contribution to the total derivative is minimized during a Lagrangian experiment (Lenschow et al. 1981). Assumptions that

are being made are that the mixed layer is uniform with height and the wind speed and the eddy transfer coefficient K are constants. If these quantities are variable the terms in equation 1 become a little more complicated, contributing to uncertainty in quantities derived from equation 1.

To visualize the whole process it is useful to draw a box with the ocean surface as the bottom of the box and the top of the boundary layer as top (Fig. 1). Assuming that the balloon moves from left to right during the period, the left hand side of the box represents the height of the boundary layer h at time t and the right hand side, h at $t + \delta t$. The 1st term on the right-hand-side of equation (1) is the vertical turbulent flux at the top of the boundary layer (evaluated at the top of the boundary layer $h = z_i$). It is the result of entrainment of air from above into the boundary layer and is equal to minus the entrainment velocity w_e (positive upwards) times the gradient in S across the top of the boundary layer. This flux can be positive or negative depending on the sign of ΔS .

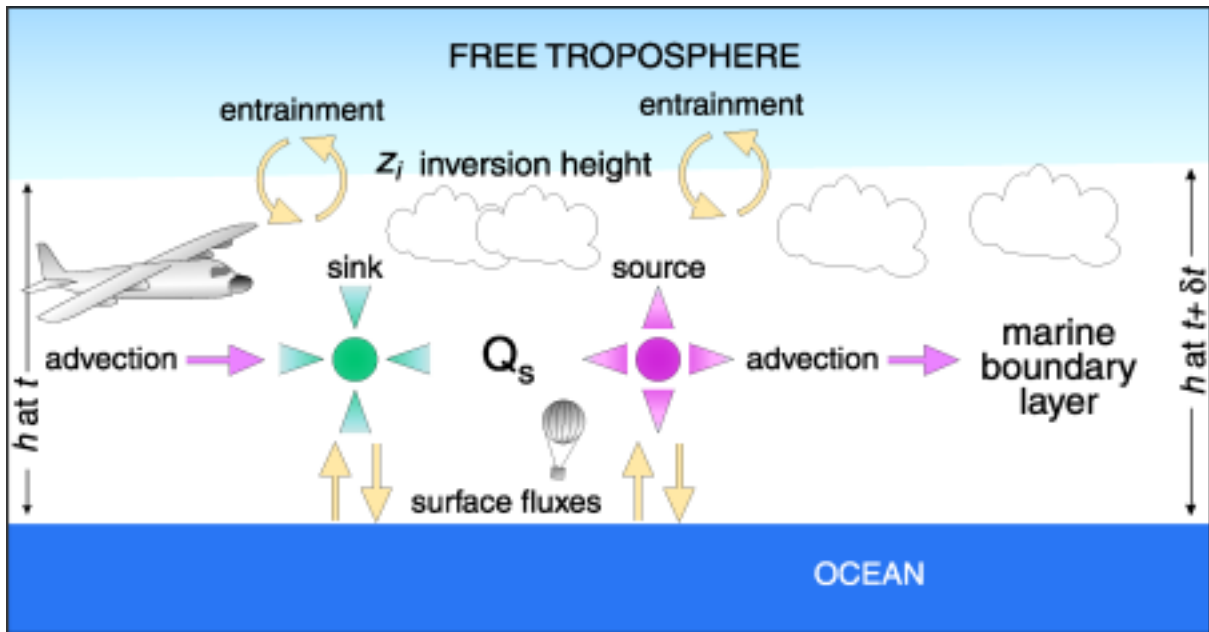


Fig. 1 Schematic illustration of the terms in the mean concentration budget for a scalar variable in the marine boundary layer with a net internal source or sink Q_s . Refer to text for explanation.

The second term, the vertical turbulent flux at the surface, is a source or sink of S at the air-earth interface and is generally measured from a trailing ship and/or estimated from satellite data. Previous field experiments have demonstrated that dispersion, the third term, is small. The fourth term is the net internal source or sink of S .

The dispersion and advection terms must be explicitly included in the error propagation analysis. Inert tracers are commonly used to estimate the impact of dispersion. The contribution due to horizontal advection (1st term) is minimized under one of two conditions: i) there is no mean vertical wind shear within the boundary layer; ii) there is mean vertical shear, but turbulent vertical circulations keep the column of air advecting at a mean rate for the mixed layer. In this latter case, the mass-weighted average horizontal velocity should be used to advect the column of boundary layer air. For a decoupled boundary layer or one with substantial cumulus convection, the vertical mixing time scale may be rather slow, perhaps of order 1 day, increasing the importance of any vertical wind shear. In timing the start of the Lagrangian experiments, care must be given in choosing synoptic conditions that optimize the success of the Lagrangian strategy and provide a trajectory accessible to aircraft sampling over an extended period.

From 1991 to the present the National Oceanic and Atmospheric Administration/Air Resources Laboratory/Field Research Division

(NOAA/ARL/FRD), in collaboration with the University of Hawaii (UH), has developed three generations of GPS balloon tracking systems for application in Lagrangian field experiments (Johnson et al. 1998). Each of these systems incorporates a constant-volume balloon in the design. Constant-volume balloons are alternatively referred to as constant-altitude balloons or constant-density balloons. For the appellation to be accurate the following conditions must be met. (i) The balloon must be filled to capacity by the time it reaches the desired flying altitude. This means that the internal pressure of the balloon must be above ambient and such that balloon skin is tightened beyond any initial elasticity. (ii) The volume of the balloon is large enough that once filled with helium it is capable of lifting the balloon and payload to the desired altitude. (iii) The strength of the external balloon shell is capable of withstanding the force exerted by the internal pressure when it reaches flying altitude. The strength of the shell must also be capable of withstanding the increased pressure due to daytime heating.

Unlike a latex weather balloon that keeps expanding as it is filled and rises in the atmosphere, a constant volume balloon shell is made of a material that maintains a constant volume and shape. In practice, any material that can be used to construct the shell has some elasticity and a thermal coefficient of expansion. Therefore, the balloon volume (and density) will change slightly with changes in

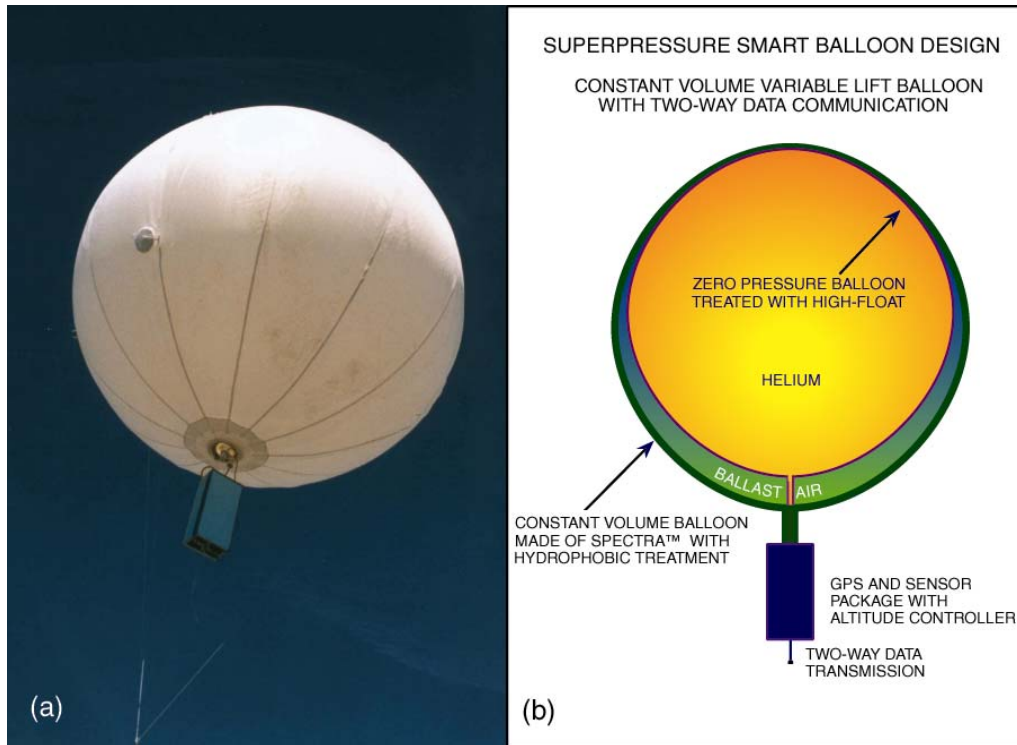


Fig. 2 (a) NOAA/UH Smart Balloon following release from the deck of the Ukrainian research ship, the Professor Vodyanitsky. (b) Sketch of the NOAA/UH Smart Balloon showing primary components.

temperature and internal pressure. Filling the constant volume balloon with helium causes the balloon to rise in the atmosphere until the mass of air displaced and the mass of the balloon payload reach equilibrium. As the temperature and barometric pressure of the surrounding atmosphere change with time, the balloon will move up or down vertically to maintain equilibrium. In addition, when the impact of precipitation, condensation, and small leaks in the balloon are considered, the value of lift controls to constrain fluctuations in balloon altitude becomes clear.

The first generation NOAA/UH balloon tracking system was deployed in the vicinity of the Azores in the Atlantic Ocean during the Atlantic Stratocumulus Transition EXperiment and the Marine Aerosol and Gas Exchange (ASTEX/MAGE) that took place in June of 1992 (Businger et al. 1996). The ASTEX design included an inexpensive tetrahedral-shaped 1.6 cubic meter Mylar® balloon (tetron), chosen for ease of construction. The ASTEX tracking system was the first to apply GPS transponders that performed very well. However, the loss of tetrons due to loading from light precipitation during the first ASTEX Lagrangian experiment reinforced the need for adding lift control to the next generation constant-volume balloon.

The second generation NOAA/UH tracking system was a *smart* tetron with an added ballast

bladder to provide adjustable lift. The adjective *smart* used here refers to the fact that the buoyancy provided by the 4.25-cubic meter Mylar® tetron automatically adjusts through the action of pumping air into or releasing air from the ballast portion of the tetron when it travels vertically outside a barometric pressure range set prior to release. The variable lift tetron and transponder were designed early in 1995 and deployed in unpolluted air south of Tasmania, Australia, during the first Aerosol Characterization Experiment (ACE-1) held in the fall of 1995 (Bates et al. 1998; Businger et al. 1998). The ACE-1 smart tetron design provided GPS location, barometric pressure, temperature, relative humidity, and tetron status data via a transponder to the NCAR C130 research aircraft flying in the vicinity of the tetrons.

The ACE-1 Lagrangian experiments investigated changes in the sulfur budget in a remote marine boundary layer (MBL) over at least a day, providing data to estimate sources, sinks, entrainment, and conversion rates for sulfur gases and aerosols (Clarke et al. 1996; Wang et al. 1998; Huebert et al. 1998). During two Lagrangian experiments (LA and LB) data were retrieved via a receiver on board the NCAR C130 research aircraft from four smart tetrons. The first of these survived more than 33 hours and was tracked during two flights of the instrumented C-130 aircraft. During LB a post-frontal air mass was tagged by three tetrons

over a 27-hour period and was sampled by a succession of three flights. Results of ACE-1 smart balloon releases indicate that the balloons were capable of adjusting lift to compensate for changes in conditions during the daytime when there was no precipitation or condensation accumulation on the surface of the balloon. However during the evening when temperatures cooled enough to cause condensation on the balloon surface, the adjustment range of the smart tetroon was insufficient to compensate for the resulting changes in tetroon-system lift.

2. The Third-Generation NOAA/UH Smart Balloon

Insights gained from the deployment of the ACE-1 smart tetroons were used in the development of a third-generation smart balloon (Fig. 2). The improved smart balloon would need to have greater dynamic lift range in order to overcome condensation or rain water loading. The increased ballast would require higher pressure inside the balloon and necessitate stronger material to withstand the increase in force on the shell of the balloon. Either a thicker, stronger and therefore heavier Mylar® film would need to be used or another material would need to be found for the shell of the balloon. After researching possible high strength materials, a plain weave Spectra® fabric was selected as the best match for the requirements of the new balloon shell. The benefits offered by Spectra® fabric include (i) very high ultimate tensile strength, (ii) very low elasticity (3% at ultimate tensile strength), (iii) light weight (0.97 gram/cc), and (iv) easy to handle. Spectra®, like any cloth fabric is easy to fold, cut and handle without damaging or puncturing. A disadvantage of the Spectra® fabric was the requirement for separate bladders inside the shell to hold the helium and air. In previous balloon designs the Mylar® outer balloon shell provided both strength and gas containment in a single layer. However the advantage of the very high strength, ease of handling, and greater durability of the Spectra® outer fabric shell made up for the required extra bladder. Standard 600-gm and 350-gm latex weather balloons were used for the outer and inner bladders.

With significantly greater balloon shell strength provided by the Spectra® fabric, the ACE-2 smart balloon is able to handle greater internal pressure and a much greater volume of air ballast. Air ballast was increased from ~160 grams for the ACE-1 project to >1200 grams for ACE-2. This added lift range proved to be essential for maintaining the balloon altitude during the ACE-2 balloon flights.

New Transponder Hardware and Software Design

The larger balloon, with greater lift capacity, made it desirable to consider a totally new transponder design. Although preliminary tests of the new balloon concepts were promising, only a few months were available for hardware and software development, testing, and fabrication prior to the field phase of ACE-2 in June of 1997.

Of the many design concerns that needed to be addressed and resolved in just a few months, energy consumption for the tracking system was paramount. Many of the new GPS receivers tested for this project were able to acquire a new position from a warm start in about 15 seconds most of the time. Previous receivers had required 40 to 60 seconds and required the same power supply current. Thus, the GPS receiver selected for this project required only a fraction of the energy required in the past.

With a larger balloon and a need to respond to conditions as quickly as possible, greater pumping capacity was needed. Two pumps were combined to provide a pumping capacity of 20 to 25 liters per minute. Pumping at this rate provides a decrease in lift at a rate of ~ 20 to 25 grams per minute. Surface evaporation rate measurements made in the lab indicated that evaporation would not take place any faster than 30 grams per minute. In a worst-case condition the balloon could rise above the desired control elevation for a short period of time.

A larger valve than used during ACE-1 was needed to release ballast air at a sufficiently fast rate to compensate for surface condensation or light precipitation. Rather than using multiple valves to switch the pumps over to pumping air out of the ballast bladder, a single large pinch-off valve on a large piece of latex rubber tubing was used. A small gear motor was used to open and close the pinch-off valve when increased lift was required. The superpressure inside the balloon forces the ballast air out of the balloon. The ballast air pumps that were used have one-way check valves that ensure there is no back flow of ballast air through the pumps. The release rate, even at low pressures, was several times the pumping rate. This allows the balloon to compensate quickly for precipitation and/or condensation that could accumulate on the balloon surface.

To reduce development time and risk to the project schedule, a popular off-the-shelf data logger was selected. Many of the software applications needed to gather data and control the operation of the balloon subsystems were a part of the data logger system functions, reducing the software development for the project from weeks or months to days. The data logger also had most of the hardware monitoring and control functions built in, which minimized the need for hardware development. Additional hardware included pump and valve on/off and

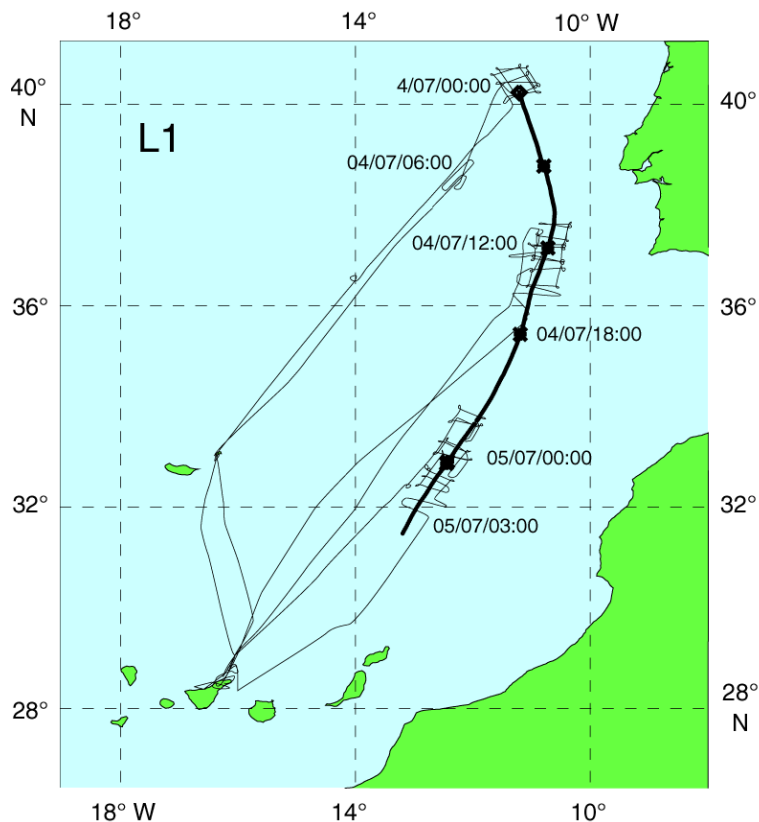


Fig. 3 Track of ACE-2 smart balloon and C-130 aircraft flight patterns during Lagrangian 1. Black symbols indicate balloon positions at synoptic times (mm/dd/hh).

open/close circuitry, the valve pinch-off system, and the switching power supply.

In previous designs, the balloon transponder was programmed or configured one time prior to release to send data back every 5 minutes, even if there was no receiver in the area. Two-way communications now allow changes in balloon operating parameters to be made after launch and transmission of data to occur only when a good link was established. The radio communications hardware was selected in conjunction with the data logger. A modem designed to interface with the data logger and a standard four-watt transceiver was used. This provided the transponder with two-way communications and reduced development time.

3. Performance of the NOAA/UH Smart Balloon during ACE-2

The Second Aerosol Characterization Experiment (ACE-2) was held from 16 June through 26 July 1997 over the Atlantic Ocean between Portugal and the Canary Islands (Raes et al. 1999). The third-generation smart balloon was deployed during three cloudy Lagrangian experiments during ACE-2 to investigate the processes that change the

chemical composition of continental aerosol in the cloudy marine boundary layer as it advects over the North Atlantic Ocean (Johnson et al. 1999).

The 68-m long Ukrainian research ship, the Professor Vodyanitskiy, was used as a launch platform for the smart balloons. When we arrived at the ship to set up and test equipment, the ship crew helped build a retractable shelter over the aft portion of the ship deck. A large reinforced plastic tarp was shipped with some of our other equipment to the port in Lisbon, Portugal. The balloon inflation shelter kept some of the wind and ocean spray off the balloon during balloon preparation in conditions of enhanced winds and heavy seas.

After three weeks of waiting for a pollution outbreak from Europe to affect the Canary Islands, a decision was made to conduct a Lagrangian experiment in a relatively clean maritime air mass. Lagrangian 1 took place from 3 to 5 July 1997. The R/V Vodyanitskiy was moved off the coast of Portugal to a position of 40° 12' N and 11° 10' W. Just before midnight on the 3 July 1997 a single smart balloon and a plume of PFC trace gas were released. Technical difficulties prevented more balloons from being released. However, the smart balloon (balloon 2) survived long enough

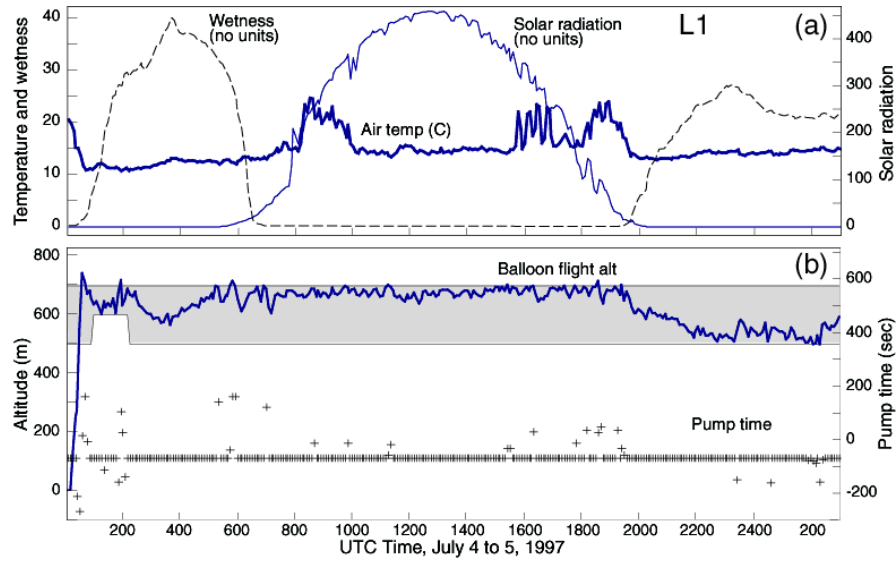


Fig. 4 Lagrangian-1 time series for balloon 2 starting at 0005 UTC on 4 July 1997 and continuing until 0245 UTC on 5 July 1997, showing Smart Balloon data, a) balloon air temperature ($^{\circ}\text{C}$), balloon wetness (no units), and solar radiation (no units), and (b) balloon height (m) and balloon pump time (s). Shaded area indicates the balloon operating window.

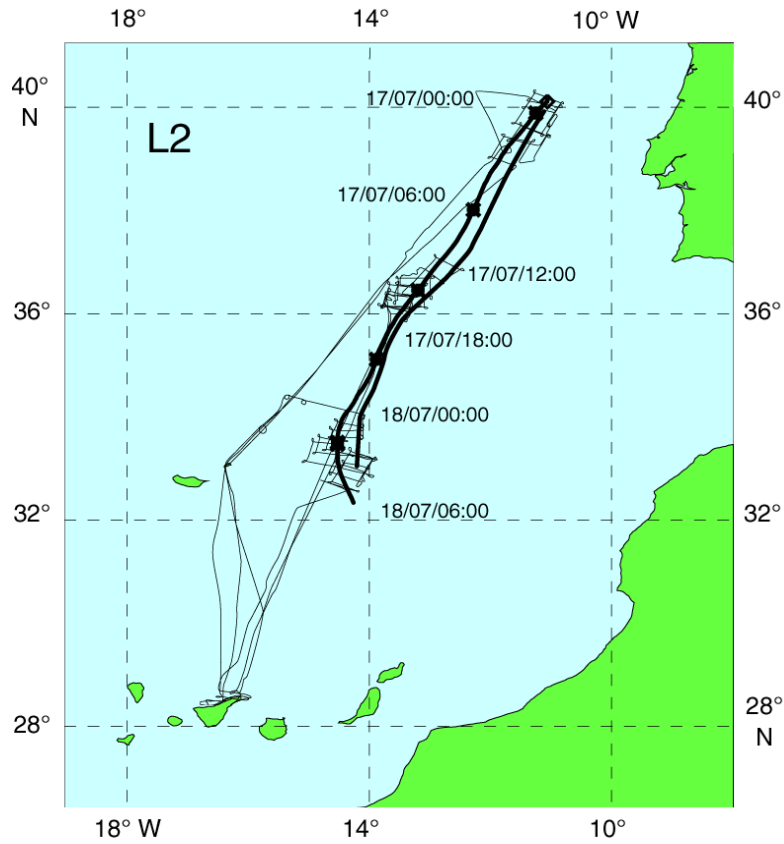


Fig. 5 Tracks of ACE-2 smart balloons and C-130 aircraft flight patterns during Lagrangian 2. Black symbols indicate balloon positions at synoptic times (mm/dd/hh).

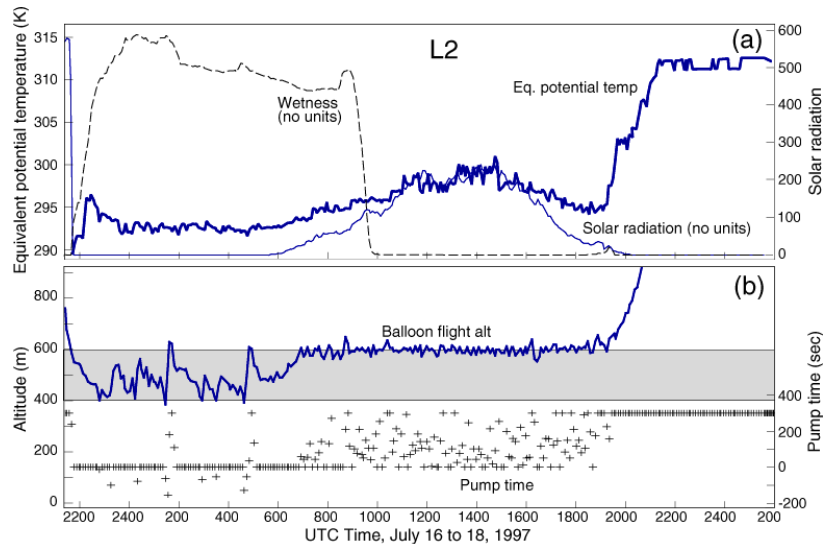


Fig. 6 Lagrangian-2 time series for balloon 4, starting at 2135 UTC on 16 July 1997 and continuing until 0155 UTC on 18 July 1997, showing Smart Balloon data, (a) balloon height (m) and balloon pump time, and (b) equivalent potential temperature (K), balloon wetness, and solar radiation (no units). Shading indicates balloon operating window.

to give more than adequate direction for the aircraft to follow the parcel of air being studied (Fig. 3).

On release the smart balloon was lofted to reside in the middle of the boundary layer, estimated to be around 500 m altitude. Early in the experiment, the balloon observer aboard the C-130 aircraft, adjusted the operating window of the smart balloon from 500-700 m to 600-700 m (Fig. 4a). The balloon transponder responded correctly by adjusting the ballast to force the balloon to stay within the narrower window. The operating window was then relaxed back to its original 500-700 m altitude range to conserve battery charge.

Initially the air parcel was advected southeast toward the African coast, but just after midday on 4 July it turned more southwesterly and was heading just to the east of Tenerife. At that time one of the engines failed on the UK Meteorological Research Flight (MRF) C-130 and the aircraft had to divert to make an emergency landing at Tenerife South airport.

Contact with balloon 2 was maintained through 0300 on 5 July and a complete data set from the balloon is available through that time. Balloon wetness and solar radiation show diurnal cycles that are out of phase (Fig 4b). Air temperature is a minimum at night and rises to maxima in the morning and afternoon as a result of direct solar radiation striking the sensor at those times. Midday air temperatures are cooler in the shade of the balloon, more closely

representing the ambient air temperature. To obtain more representative measurements in future, balloon designs will need to include aspirated temperature and humidity sensors that are shielded from direct solar radiation.

The C-130 aircraft flew three sorties of approximately 9 hours each and separated by about 3 hours ground time for refuelling and servicing. The last flight was somewhat foreshortened due to the engine failure. By then sufficient data had been collected to document the evolution of the aerosol in the air parcel over a 30-hour period. The CIRPAS Pelican aircraft carried out a fourth flight in the vicinity of Tenerife but was unable to locate the balloon, leaving some uncertainty whether they were sampling in the same air parcel (Fig. 3).

Lagrangian 1 was carried out in a relatively clean maritime air mass and provides a very good data set for comparison with the other two Lagrangians that were in polluted, continental air masses. Lagrangian 1 produced the largest changes in aerosol characteristics of the three experiments undertaken. See Johnson et al. (1999) for an overview of the evolution of the marine boundary layer and the cloud and aerosol microphysics during the three cloudy ACE-2 Lagrangian experiments.

The second Lagrangian was undertaken 16-18 July 1997 within a polluted continental air mass advecting from over northern France with significant stratocumulus cloud cover experienced throughout. Light drizzle was experienced at times. Two balloons (balloons 4 and 5) were successfully released on 16 July

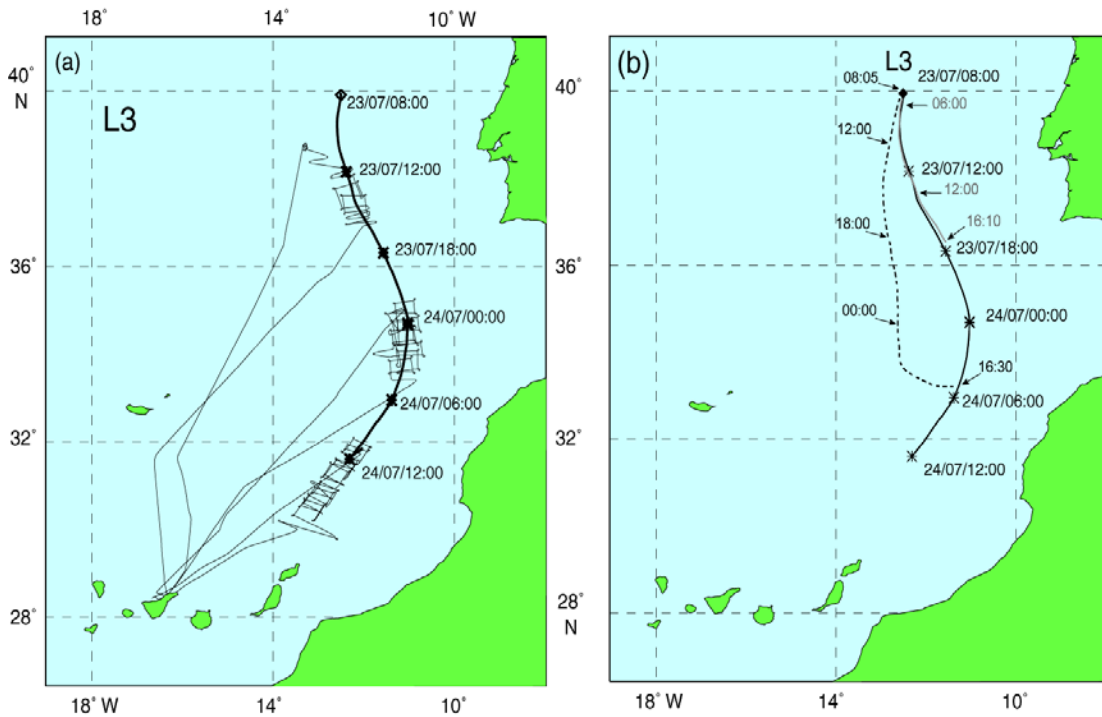


Fig. 7 (a) Track of ACE-2 smart balloon 8 and C-130 aircraft flight patterns during Lagrangian 3. Labeled symbols indicate balloon positions at synoptic times (month/day/hour) (b) Tracks of balloon 7 (gray line), balloon 8 (black line), and balloon 9 (dashed line) during Lagrangian 3. Location times (UTC) are indicated with labeled arrows for balloons 7 and 9, and date and times are given for balloon 8 (month/day/hour).

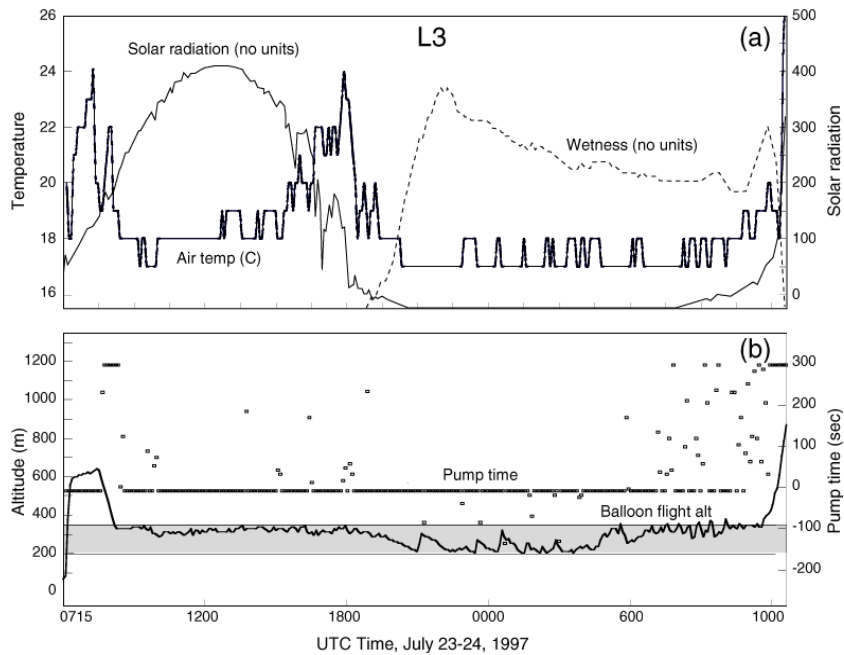


Fig. 8 Lagrangian-3 time series for balloon 8, starting at 0715 UTC on 23 July 1997 and continuing until 1030 UTC on 24 July 1997, showing Smart Balloon data, a) balloon air temperature ($^{\circ}$ C), balloon wetness (no units), and solar radiation (no units), and b) balloon height (m) and balloon pump time (s). Shaded area indicates the balloon operating window.

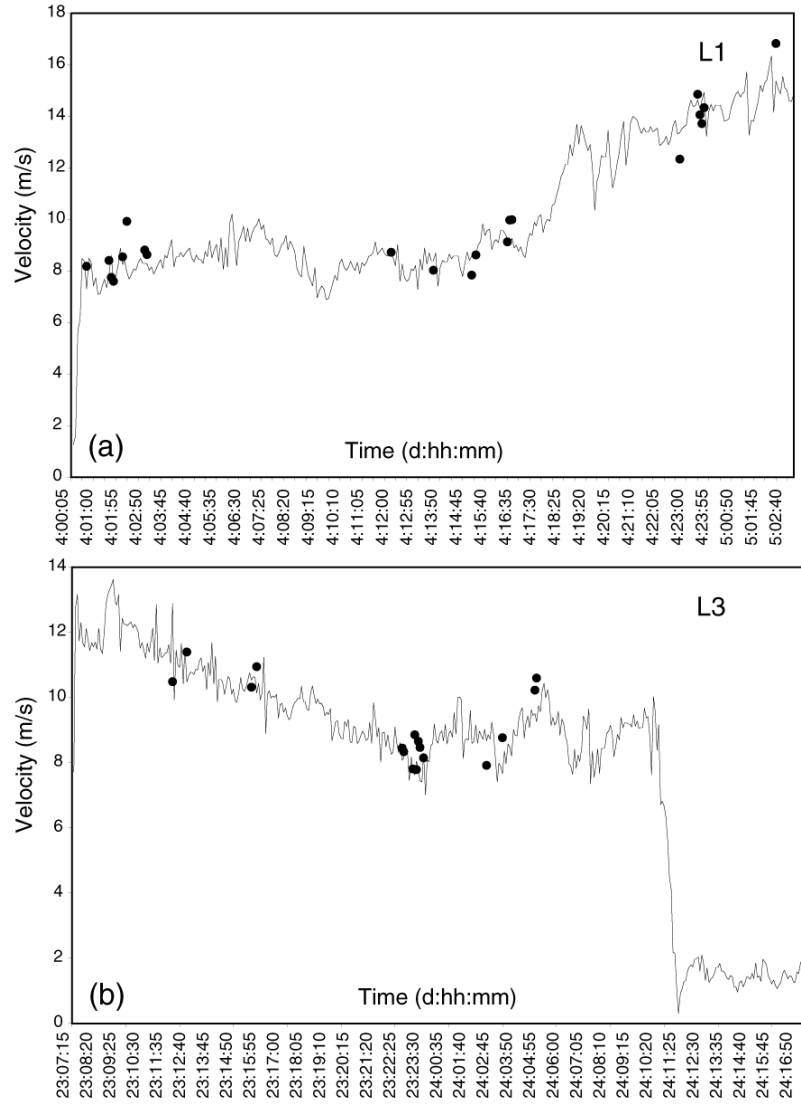


Fig. 9 Comparison of smart balloon velocity (line) to C-130 Aircraft flight level wind speed (m s⁻¹) for Lagrangian 1 (balloon 2) and Lagrangian 3 (balloon 8).

1997 at 2200z and 2300z from the deck of the R/V Vodyanitskiy located at 40° 10'N, 11° 04'W (Fig. 5). Three flights of the C-130 were carried out in pursuit of the balloons. Despite changes in solar radiation and balloon wetness, the balloons tracked within the prescribed altitude limits within the marine boundary layer until ~2100 UTC on 17 July (Fig. 6). Time series of temperature and humidity allowed equivalent potential temperature to be retrieved (Fig. 6b). At this time both balloons began to rise into the free troposphere because of slow leaks of ballast air from their bladders. Subsequent tests revealed the leaks to be due to stretching of the rubber bladder against the seam in the Spectra® shell, under conditions of prolonged superpressure.

The third Lagrangian took place on 23 and 24 July 1997 in a polluted continental air mass that originated over central northwest Europe. Three smart balloons were released at 0615z, 0730z and 0815z on 23 July 1997 from the deck of the RV Vodyanitskiy located near 40° N, 120° 30'W (Fig. 7). Of the three balloons, the first (balloon 7) failed ~ 12 hours after release, perhaps because of a transponder failure. The second (balloon 8) operated successfully until 1000z on 24 July 1997 (Fig. 7a). The third failed on release (balloon 9) apparently because of a puncture in the ballast bladder that caused the balloon to rise into the free troposphere soon after release. The balloons were each set up to drift at the estimated midpoint of the marine boundary layer (~300 m). The tracks of balloons 7 and 8 remained very close to the prescribed

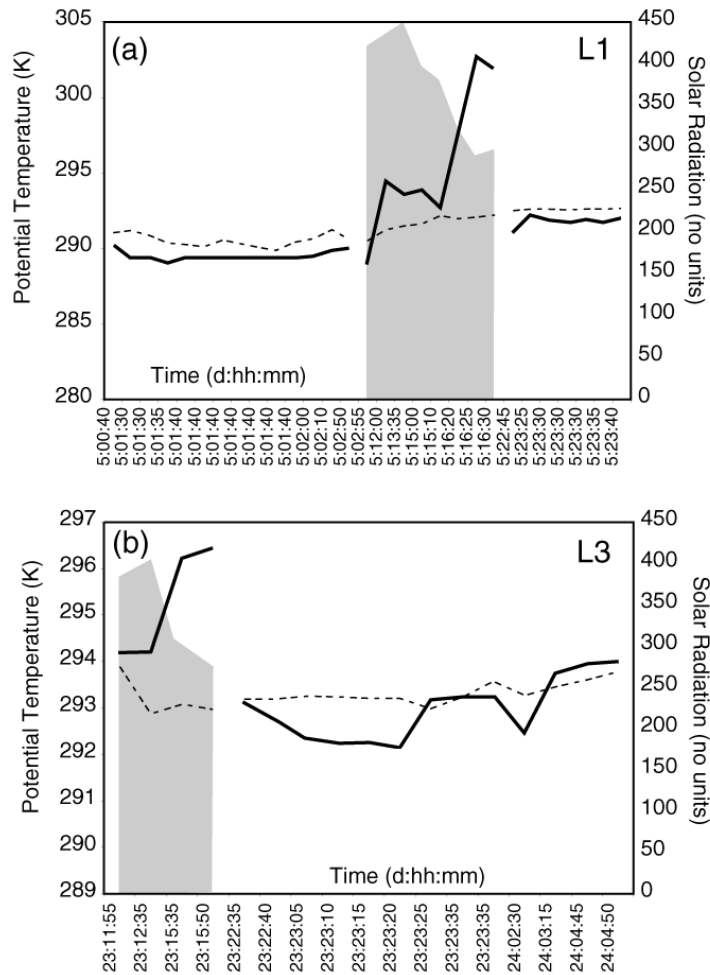


Fig. 10 Time series of potential temperature K (heavy solid line = balloon, dashed line = C-130 flight level) and balloon measured solar radiation (shaded) for (a) Lagrangian 1 (balloon 2) and (b) Lagrangian 3 (balloon 8). Data gaps indicate times between C-130 flights.

altitude and to each other (Fig. 7b), whereas the track of balloon 9, which quickly rose to an altitude of ~ 625 mb, diverged from the other two tracks. Balloon 8 maintained altitude and provided a full suite of data (Fig. 8). As with previous smart-balloon time series, solar radiation and balloon wetness are out of phase (Fig. 8b). The cloud conditions during Lagrangian 3 included a mixture of broken cumulus and stratocumulus clouds. It appears that the balloon entered cloud and remained there for ~ 12 hours (Fig. 8b). The structure of the boundary layer and pollution layer in this experiment were highly complex, in complete contrast to the aerosol characteristics evolution, which was rather simple (Johnson et al. 1999). Surprisingly, dramatic changes to the thermodynamic structure of the polluted lower

atmosphere were accompanied by only modest changes in the aerosol characteristics.

Comparison of Balloon Data with Aircraft Data and Model Output

Balloon position data were used to calculate the propagation velocity of the balloon. The resulting balloon velocity data were compared with C-130 flight-level wind data to assess how well the NOAA/UH smart balloons tracked with the air in which they were embedded (Fig. 9). To remove the potential bias associated with vertical wind shear, flight level data within ± 5 mb of the same pressure level as measured by the balloon were used in the comparison. The close correlation between the balloon calculated and aircraft measured velocities is shown in Fig. 9. The RMS

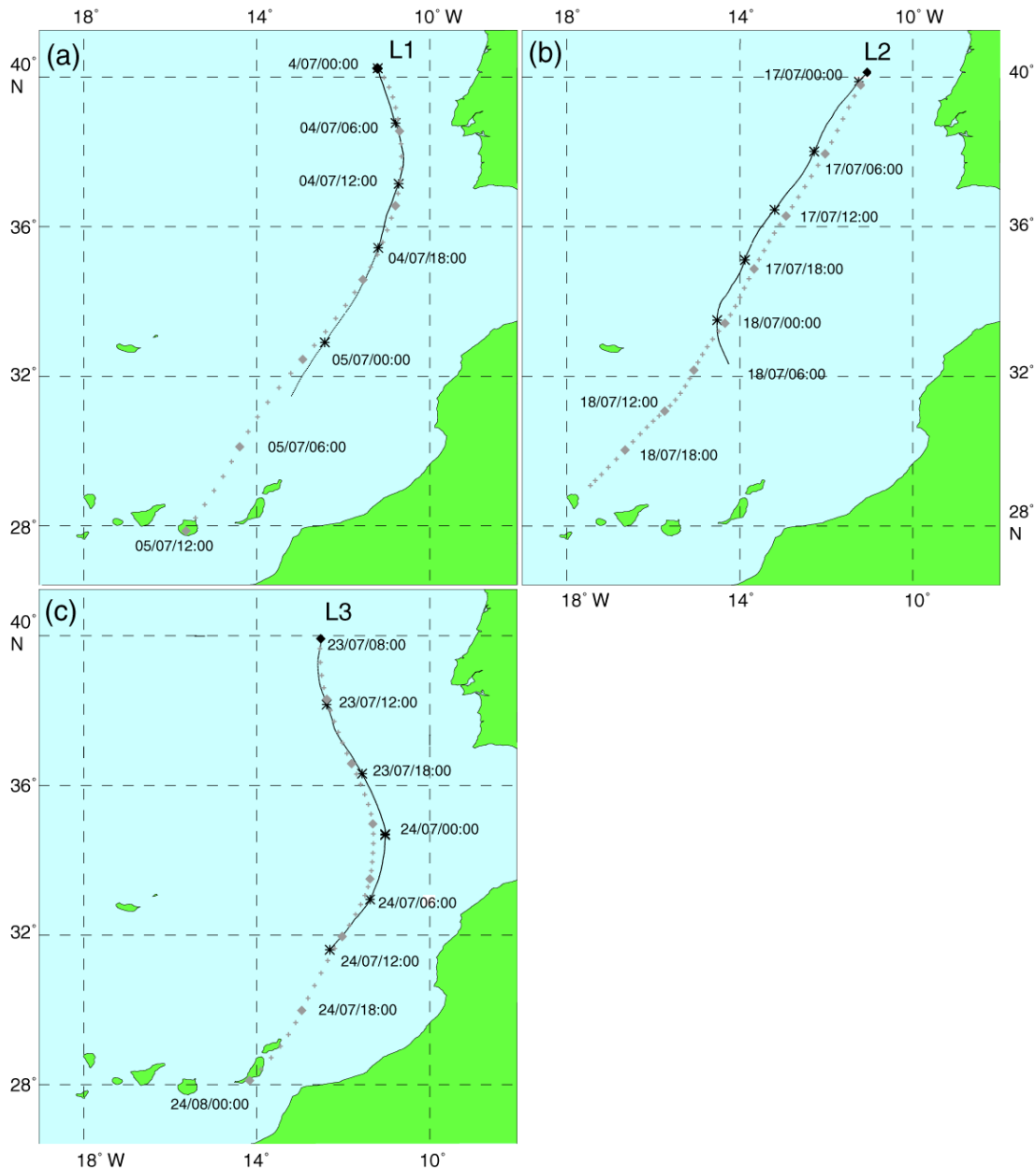


Fig. 11 Tracks of ACE-2 smart balloons (thin lines) and GSM constant altitude trajectories for 500 m above sea level (gray crosses) during (a) Lagrangian 1, (b) Lagrangian 2, and (c) Lagrangian 3. Labeled symbols indicate balloon and model trajectory positions at synoptic times (month/day/hour).

difference between the velocity observed by aircraft and calculated from balloon motion is 0.75 m s^{-1} for L1, 1.75 m s^{-1} for L2, and 0.96 m s^{-1} for L3, respectively. The slightly larger RMS value for L2 may be attributed to a slightly greater difference in vertical position between the C-130 and the balloon than observed in the data for L1 and L3. Nevertheless, these differences are smaller than the errors associated

with the wind measurements themselves, and lend confidence to the assertion that the balloons travel with the speed of the air in which they are imbedded.

The balloon potential temperature data were compared with observations taken by the C-130 (Fig. 10). The results reveal a radiation bias in the balloon temperature measurements, with a positive bias (balloon warmer than C-130)

during the day and a negative bias at night. The largest bias occurs during the afternoons when the balloon no longer shades the instrument package and solar radiation directly strikes the instruments (e.g., Figs. 4 and 10a). This finding suggests the need for aspirated sensors on future generations of the smart balloon.

Trajectory simulations were constructed using output from the National Center for Environmental Prediction - Global Spectral Model (NCEP GSM) (Kalnay et al. 1990) to evaluate the ability of the GSM to predict the observed smart balloon tracks (Fig. 11). Results of the comparison of model and balloon trajectories are presented to evaluate the ability of numerical weather prediction (NWP) models to predict the observed smart balloon tracks and assess the potential utility of model trajectory simulations in planning future field experiments. Forward trajectories of the NCEP Global Spectral Model (GSM) are based on the aviation run. The GSM has 28 sigma levels in the vertical and a horizontal resolution of ~111 km. The lowest pressure level is at ~995 mb. Trajectories were calculated using the HY-SPLIT (HYbrid Single Particle Lagrangian Integrated Trajectory) Model (Draxler 1992) applied to GSM hourly output over 16 sigma surfaces at the midpoints of layers that vary in thickness from ~35mb at the surface to ~54mb thick at the model upper boundary. The three dimensional gridded GSM output values for u and v were input as initial velocities and vertical velocity, w , was integrated using vertical integration of horizontal velocity divergence. Using these variables, along with parcel latitude, longitude and height, z , above model terrain, trajectories were computed using a simple first-order approximation taking into account curvature in the wind field. Finally, application of a bilinear interpolation from the data grid defined meteorological variables at the parcel position.

The model trajectories shown in this section were initialized at a time near the release time for the balloons and are calculated for a constant altitude of 500 m, corresponding to a model level closest to that of the smart balloons. For flight-planning purposes, output from a model run at least 12 hours previous to the release time of marker balloons would be needed. It is implicit that model resolution and quality and quantity of the data available for the initial condition of the model runs are factors that need to be considered when making trajectory comparisons. ACE2 benefits from the fact that the Northern Hemisphere is relatively

data rich. The results shown here, therefore, may be considered a best-case GSM simulation.

A comparison of the tracks of the ACE-2 smart balloons with GSM trajectories (Fig. 11) shows good agreement. For L1 the GSM winds move the air parcel farther than is observed, with the largest discrepancy (86 km) occurring during the evening of 4 July (04/07/1800 in Fig. 11a). At all times, the model trajectory error, which ranges from 24 to 86 km, is smaller than the model resolution (~111 km). The best performance of the GSM is during L2, in which the model error ranges from 24 to 36 km and averages 31 km (Fig. 11b). The model forecast trajectory for L3 is also very good. In this case the motion of the balloon is under forecast and the error ranges from 43 to 60 km (Fig. 11c). The ability of the GSM to provide reasonable simulations of the balloon trajectories benefits from the good initial condition provided by sufficient upstream observational data in the Northern Hemisphere. Relatively stable atmospheric conditions during the Lagrangian experiments and the lack of divergence seen in the trajectories of balloons 4 and 5 (Fig. 5) and balloons 7 and 8 (Fig. 7b), also improve the ability of the GSM to correctly simulate the trajectory. Comparisons of the balloon trajectories with trajectory forecasts from mesoscale NWP models with higher spatial and temporal resolution will likely result in even smaller forecast trajectory errors. Such comparisons are currently being undertaken and are beyond the scope of this paper.

4. Conclusions and Future Development

A third-generation smart balloon was designed at NOAA Air Resources Laboratory Field Research Division, in collaboration with the University of Hawaii, for deployment during the ACE-2 field program. Development of the improved smart balloon relied on insights gained from the deployment of a first generation smart tetraon during ACE-1. All major components of the ACE-2 Lagrangian tracking balloon were updated and improved. Significant design improvements include (i) a stronger outer shell to significantly increase dynamic lift range, (ii) two way radio communication with the balloon to allow interactive control of the balloon operating parameters by an observer, and (iii) a spherical design to reduce exposure to precipitation.

Overall the smart balloons performed very well during the ACE-2 Lagrangian experiments. The GPS receiver acquired position ~ 3 times faster than previous versions. The two-way communications worked well and provided operating flexibility not available during previous field experiments. The balloon altitude control worked flawlessly to

overcome environmental impacts on balloon buoyancy due to solar radiation and precipitation on the balloons.

The ACE-2 smart balloons, however, did encounter problems with the external air ballast bladder. The ballast bladder developed slow leaks after prolonged exposure to superpressure. The loss of ballast air caused the balloon to rise in altitude above the marine boundary layer after a day or longer, where they were no longer representative of the position of the air parcel of interest. The source of the problem has been identified and a solution has subsequently been developed and successfully tested.

Comparisons of flight-level data from the C-130 and balloon data show good agreement between the observations, and help confirm that the balloons are tracking the air in which they are embedded. A similar air temperature comparison shows a radiation bias in the balloon sensor, suggesting the need for aspiration in future generations of the smart balloon. Comparisons of the balloon trajectories with forecast trajectories from the HY-SPLIT model, using GSM forecast wind data, show errors that were smaller than the resolution of the GSM output. Results using winds output from a mesoscale NWP model will likely further reduce the position errors, suggesting that future Lagrangian experiments could perhaps be undertaken using forecast trajectories in conjunction with released tracers.

Work is progressing on several fronts to improve the performance of smart balloons. Transponder design changes are being considered that will allow the transponder to fit inside the balloon. This will simplify balloon launch, reduce overall weight of the transponder, offer greater protection from moisture and direct solar radiation, and will physically protect the transponder from damage during and after launch. The feasibility of using small-footprint inflation tubes is being investigated. The tubes can be scattered around the deck of a ship to allow near simultaneous release of multiple tracking balloons. The inflation tubes will provide protection from the wind, rain, and salt spray while the balloon is inflated and lift is set. After inflation, the inflation tube top is pulled back and it becomes a launch tube.

In the past pontoons attached to a long line have been used to help protect the balloon and transponder from going into the ocean if the balloon becomes overloaded with precipitation. Experience in ACE-2 suggests that such ballast pontoons can be eliminated, saving on weight and simplifying launch, with minimal risk of having the balloon impact the ocean.

The Iridium Satellite phone system became operational in the fall of 1998. Cost estimates make this an attractive option and costs will no doubt decrease with time as the system gains participation.

With satellite telephone communication, smart balloons can be tracked and controlled over the most remote locations even when no aircraft are in the area, significantly increasing the flexibility of the balloon platform's application.

In summary the NOAA/UH smart balloon design provides the means to track a parcel of air at the desired altitude by varying the density of the balloons as environmental conditions demand. The dynamic range afforded by the high strength spherical shell and the lift control in the ACE-2 design allows the balloons to remain within desired altitude operating limits despite the impacts of condensation, rainfall, and radiative cooling. A suite of lightweight instruments borne by future smart balloons can provide useful in situ and radiometric meteorological data. The in situ data combined with the balloon's dynamic range enable the balloon transponder to be programmed to remain at a constant altitude, to follow an isobaric or isentropic surface, or to perform vertical soundings. With the availability of satellite data telemetry it becomes feasible to remotely control the balloon flight anywhere on the globe in the absence of proximate aircraft. These capabilities and the economical cost of the design make the smart balloon an attractive platform for a broad range of future applications in the atmosphere.

ACKNOWLEDGMENTS

We are grateful to Shane Beard and John Heyman for assistance in the field. We are indebted to Roger Carter who provided programming support for the transponder design. Karsten Suhre was helpful in providing needed C-130 data. We appreciate the constructive comments of Dr. J. A. Businger and two anonymous reviewers that contributed to the final manuscript. Nancy Hulbert contributed to the final graphics. This research is a contribution to the International Global Atmospheric Chemistry (IGAC) Core project of the International Geosphere-Biosphere Programme (IGBP) and is part of the IGAC Aerosol Characterization Experiments (ACE). Mylar® is a registered trademark of Dupont. Spectra® is a registered trademark of Allied Signal. This work is supported by the National Science Foundation under grants ATM94-19536 and ATM96-10009 and ONR grant N00014-92-J-1285. SOEST contribution xxxx.

REFERENCES

Bates, T.S., B.J. Huebert, J.L. Gras, F. B. Griffiths and P.A. Durkee, 1998: The International Global Atmospheric Chemistry (IGAC) Project's First Aerosol Characterization Experiment (ACE-1) - Overview, *J. Geophys. Rev.*, 16,297-16,318.

- Businger, S., S.R. Chiswell, W.C. Ulmer, and R. Johnson, 1996: Balloons as a Lagrangian Measurement Platform for Atmospheric Research, *J. Geophys. Res.*, **101**, 4363-4376.
- Businger, S., R. Johnson, J. Katzfey, S. Siems, and Q. Wang, 1998: Smart Tetroons for Lagrangian Air Mass Tracking During ACE-1. *J. Geophys. Res.*, In press.
- Clarke A.D., T. Uehara, and J.N. Porter, 1996: Lagrangian evolution of an aerosol column during the Atlantic Stratocumulus Transition Experiment, *J. Geophys. Res.*, **101**, 4351-4362.
- Draxler, R.R., 1992: *Hybrid single-particle Lagrangian integrated trajectories (HYSPPLIT): Version 3.0 - User's guide and model description*. NOAA Tech. Memo. ERL ARL-195 [Available from the National Technical Information Service, 5285 Port Royal Road, Springfield, VA 22161].
- Huebert, B.J., S.G. Howell, L. Zhuang, J. Heath, M. Litchy, D.J. Wylie, J. Kreidler, S. Coeppicus, and J. Pfeiffer, 1998: Filter and impactor measurements of anions and cations during ACE-1. *J. Geophys. Res.*, **103**, 16,493-16,510.
- Johnson, D.W., S. Osborne, R. Wood, K. Suhre, R. Johnson, S. Businger, P.K. Quinn, A. Wiedensohler, P.A. Durkee, L.M. Russell, M.O. Andreae, C. O'Dowd, K. Noone, B. Bandy, J. Rudolph, and S. Rapsomanikis, 1999: An Overview of the Lagrangian Experiments Undertaken During the North Atlantic Regional Aerosol Characterization Experiment (ACE-2). *Tellus*, In review for this ACE-2 Special Issue.
- Johnson, R., R. Carter, and S. Businger, 1998: Evolution of Smart Balloon Design for Lagrangian Air Mass Tracking. *GPS World*, **9**, 33-38.
- Kalnay, M., M. Kanamitsu, and W.E. Baker, 1990: Global numerical weather prediction at the National Meteorological Center. *Bull. Amer. Meteor. Soc.*, **71**, 1410-1428.
- Lenschow, D. H., R. Pearson, Jr., and B. B. Stankov, 1981: Estimating the ozone budget in the boundary layer by use of aircraft measurements of ozone eddy flux and mean concentration, *J. Geophys. Res.*, **86**, 7291-7297.
- Raes, F., T. Bates, G. Verver, D. Vogelenzang, M. Van Liedekerke, 1999: The Second Aerosol Characterization Experiment (ACE-2): Introduction, meteorological overview, and main results. *Tellus*, in review for this ACE-2 special issue.
- Seinfeld, J.H., Hecht, T.A., and Roth P.M., 1973: Existing needs in the observational study of atmospheric chemical reactions, U.S. E.P.A. Report EPA-R4-73-031.
- Suhre, K., C. Mari, T.S. Bates, J.W. Johnson, R. Rosset, Q. Wang, A.R. Bandy, D.R. Blake, S. Businger, F.L. Eisele, B.J. Huebert, G.L. Kok, R.L. Mauldin, A.S. Prevot, R.D. Schillawski, D.J. Tanner, and D.C. Thornton, 1998: Physico-chemical modeling of the First Aerosol Characterization Experiment (ACE-1) Lagrangian B 1. A moving column approach. *Journal of Geophysical Research*, **103**, 16,433-16,455.
- Wang, Q., K. Suhre, P. Krummel, S.T. Siems, L. Pan, T.S. Bates, J.E. Johnson, D.H. Lenschow, B.J. Huebert, G.L. Kok, R.D. Schillawski, and S. Businger, 1998: Characteristics of the marine boundary layers during Lagrangian measurements, Part I: General conditions and mean vertical structure. *J. Geophys. Res.*, In press.
- Zak, B. D., 1983: Lagrangian studies of atmospheric pollutant transformations. In *Trace Atmospheric Constituents: Properties, Transformations, Fates*, John Wiley & Sons, 303-344.